Psychopharmacology

Original Investigation

DNA damage and ubiquitinated neuronal inclusions in the substantia nigra and striatum of mice following MDMA (ecstasy)

F. Fornai[1, 2] , P. Lenzi[1], G. Frenzilli[1], M. Gesi[1], M. Ferrucci[1], G. Lazzeri[1], F. Biagioni[2], M. Nigro[1], A. Falleni[1], M. Giusiani[3], A. Pellegrini[1], F. Blandini[4], S. Ruggieri[2] and A. Paparelli[1]

(1) Department of Human Morphology and Applied Biology, University of Pisa, 56126 Pisa, Italy

(2) I.R.C.C.S., I.N.M. Neuromed Pozzilli (IS), Italy

(3) Department of Public Health, University of Pisa, Pisa, Italy

(4) I.R.C.C.S. Istituto Neurologico C. Mondino, Pavia, Italy

F. Fornai
Email: f.fornai@med.unipi.it
Phone: +39-050-835927-2218611
Fax: +39-050-2218606

Received: 26 August 2003 **Accepted:** 4 November 2003 **Published online:** 13 December 2003

Abstract

Rationale 3,4-Methylenedioxymethamphetamine (MDMA) is an amphetamine derivative,

which is neurotoxic to both serotonin (5HT) and dopamine (DA) nerve terminals. Previous reports, carried out in rodents and non-human primates, demonstrated neurotoxicity to monoamine axon terminals, although no study has analyzed nigral and striatal cell bodies at the sub-cellular level.

Objective In this study, we examined intrinsic nigral and striatal cells, and PC12 cell cultures to evaluate whether, in mice, MDMA might affect nigral and striatal cell bodies.

Methods After administering MDMA, we analyzed effects induced in vivo and in vitro using high-performance liquid chromatography (HPLC) analysis, light- and electron microscopy with immunocytochemistry, and DNA comet assay.

Results We found that MDMA (5 mg/kg ×4, 2 h apart), besides a decrease of nigrostriatal DA innervation and 5HT loss, produces neuronal inclusions within nigral and intrinsic striatal neurons consisting of multi-layer ubiquitin-positive whorls extending to the nucleus of the cell. These fine morphological changes are associated with clustering of heat shock protein (HSP)-70 in the nucleus, very close to chromatin filaments. In the same experimental conditions, we could detect oxidation of DNA bases followed by DNA damage. The nature of inclusions was further investigated using PC12 cell cultures.

Conclusions The present findings lead to re-consideration of the neurotoxic consequences of MDMA administration. In fact, occurrence of ubiquitin-positive neuronal inclusions and DNA damage both in nigral and striatal cells sheds new light into the fine alterations induced by MDMA, also suggesting the involvement of nuclear and cytoplasmic components of the ubiquitin-proteasome pathway in MDMA toxicity.

Keywords 3,4-Methylenedioxymethamphetamine - Basal ganglia - Comet assay - Neuronal inclusions - Neurotoxicity - Heat-shock protein (HSP)-70 - Ubiquitin-proteasome system - Immuno-electron microscopy - Whorls

---

Introduction

3,4-Methylenedioxymethamphetamine (MDMA, ecstasy) is widely abused in the Western World, where a large number of young subjects take the drug in a recreational context (Parrott et al. *2001*; Pope et al. *2001*; Strot et al. *2002*; Lyles and Cadet *2003*). Knowledge on the neurobiology of MDMA is growing rapidly. It is widely established that, early after MDMA administration, there is a marked increase in oxidative species producing both

lipid peroxidation and depletion of antioxidant systems, such as Cu/Zn superoxide dysmutase activity in specific brain regions including the neostriatum (Gibb et al. *1990*; Jayanthi et al. *1999*). Increase in the production of oxidative species within affected neurons is considered as a critical step in mediating MDMA neurotoxicity (Gibb et al. *1990*). In particular recent studies demonstrate that MDMA produces an increase of free radicals, which are implicated in the neurotoxic effects (Green et al. *2003*), while oxidative stress produced by MDMA underlies the process of neurotoxicity at the level of axon terminals (Gudelsky and Yamamoto *2003*). Interestingly, oxidative stress and increase of free radicals were recently reported in human MDMA abusers (Zhou et al. *2003*). Most of the studies carried out in animal models focused on the effects at the level of monoamine axon terminals.

In the present study, we evaluated in C57 Black mice whether consequences of MDMA-induced oxidation might extend to the cell body and the nucleus of the cell undermining DNA integrity. In particular, in order to detect oxidation to DNA basis and potential DNA damage we used the novel approach of single-cell gel electrophoresis (comet assay) in the substantia nigra and striatum. Among various proteins which are connected with DNA oxidative stress, heat shock protein-70 (HSP-70) is considered to play a seminal role in protecting and repairing chromatin filaments (Abe et al. *1995*; States et al. *1996*; Sherman and Goldberg *2001*). Therefore, we decided to evaluate whether MDMA administration produces variations in heat shock protein-70 (HSP-70) immunoreactivity. Again, oxidative damage is known to produce misfolded proteins which are degraded via the ubiquitin-proteasome system (Sherman and Goldberg *1996, 2001*). This multi-enzymatic catalytic pathway is activated via ubiquitination of substrates and it is implicated in the formation of ubiquitin-positive neuronal inclusions. In order to investigate whether MDMA-induced sub-cellular alterations might lead to an involvement of the ubiquitin-mediated catalytic pathways, we evaluated the occurrence of ubiquitin-positive inclusions within the nucleus and cytoplasm of dopamine (DA) nigral cell bodies and striatal gamma-aminobutyric acid (GABA) neurons. As a further step, we tried to reproduce the same phenomena in a simpler in vitro model (PC12 cells) in order to analyze the dynamic and the fine structure of inclusions.

Materials and methods

Animals, experimental design, MDMA

purification and authenticity assay

Male C57 Black mice (C57BL/6 J), 11–12 weeks old, were obtained from Harlan (San Pietro al Natisone, Italy). In the animal facility, mice were fed ad libitum and kept under closely controlled environmental conditions (12-h/12-h light/dark cycle, with lights on between 0700 hours and 1900 hours). As the toxicity of amphetamine derivatives is highly variable, critically depending on room temperature and number of animals per cage, mice were constantly kept at 21°C and housed one per cage. Mice were treated in accordance with the Guidelines for Animals Care and Use of the National Institutes of Health. All procedures were approved by the local Animal Care Committee.

The day of the experiment, mice received consecutive i.p. injections of MDMA hydrochloride (5 mg/kg ×4, 2 h apart) or saline (controls). We obtained authentic MDMA hydrochloride from solid samples (Institute of Forensic Toxicology, Prof. M. Giusiani). Briefly, solid samples were ground to a powder and dissolved with diluted hydrochloric acid and crystallized twice. The purity of the chloride-containing crystals was verified before the experiments by measuring the melting point and by running gas chromatography (GC) and mass spectrometry, which demonstrated the authenticity and purity of MDMA (Fig. 1).

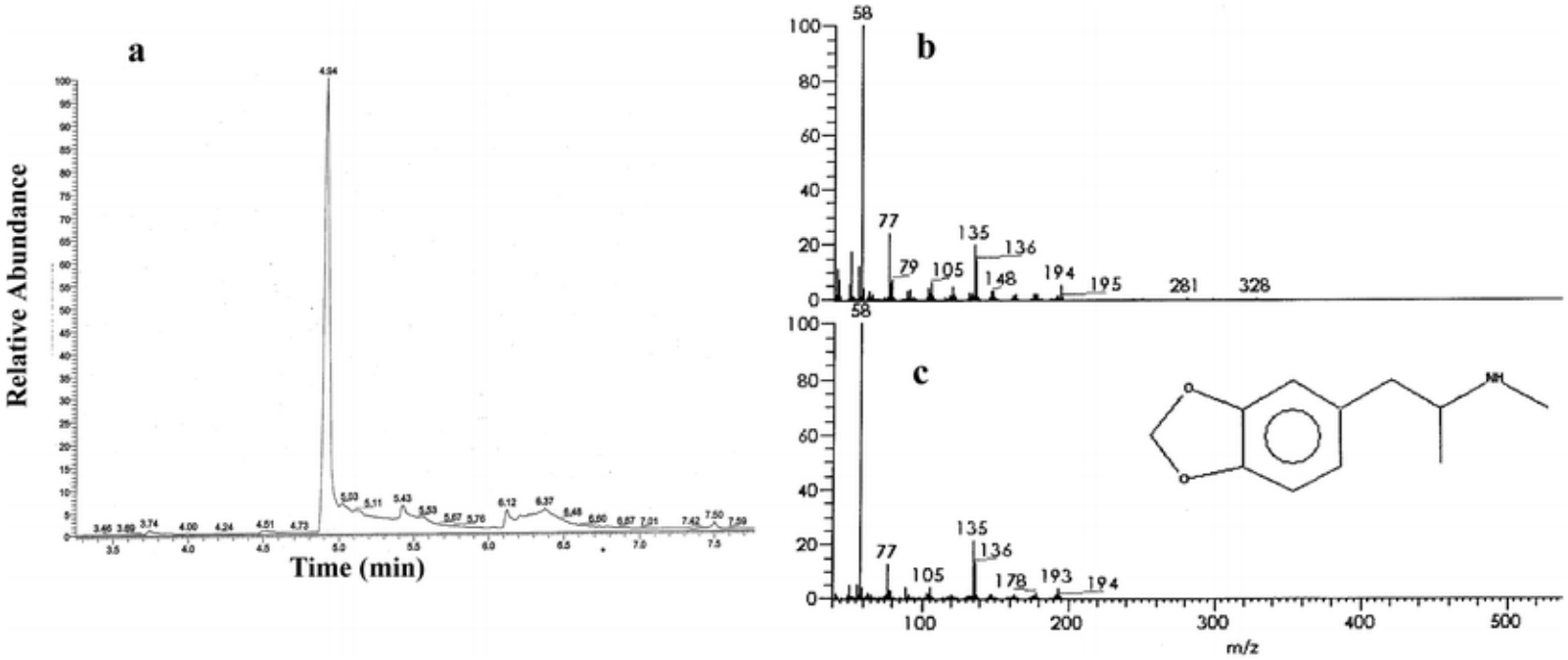

Fig. 1 Separation and identification of authentic methylenedioxymethamphetamine (MDMA; ecstasy) used in the experiments. **a** Gas chromatography showing a single peak corresponding to purified MDMA. Mass spectrum of the purified compound (**b**) overlaps with the MDMA spectrum obtained from the NIST library (**c**) where the molecular structure of the mass spectrum, corresponding to MDMA, is shown

Mice were sacrificed 7 days later, except for one group which was sacrificed immediately after the last MDMA injection to measure the DNA damage and bases oxidation early after MDMA administration. Mice used for the morphological (light and electron microscopy with or without immunostaining) section of the study were perfused with paraformaldehyde/glutaraldehyde, while mice used for the biochemical analysis and comet assay were killed by decapitation. For each procedure, groups were composed of 7–10 mice.

Biochemical assays

After decapitation, samples were processed depending on the specific analysis. For monoamine assay, the brains were rapidly removed and placed on ice-cold saline. The striatum was dissected out through the external wall of the lateral ventricle, while the substantia nigra was obtained by micro-punching. Monoamines were measured by means of high-performance liquid chromatography (HPLC) with a reverse-phase column (250×4.5 mm, C18, SGE) and two coulometric electrochemical detectors, as previously described (Fornai et al. *1999*). The mobile phase consisted of a citrate-phosphate buffer (0.04 M citric acid, 0.06 M Na_2HPO_4 $2H_2O$) solution containing 0.1 mM ethylene diamine tetraacetic acid (EDTA), 0.6 mM 1-heptanesulphonic acid sodium salt, and 10% methanol.

The standard curve for each compound was calculated using regression analysis of the ratios of the peak areas for various concentrations of each compound recorded at the reducing electrode.

Comet assay

DNA integrity was evaluated by the use of alkaline single cell gel electrophoresis (SCGE) or comet assay, according to Singh et al. (*1988*) with minor modifications.

Briefly, isolated cells were embedded in agarose on a microscope slide, lyzed with detergent and high salt. The technique is based on the principle that any break in the DNA causes the supercoiling to relax locally, allowing negatively charged loops of DNA to freely extend and migrate with any short fragments, in the electric field, toward the anode as a "comet tail".

After sacrifice, separate specimens from the two brain areas of interest (striatum and substantia nigra) were washed in cold PBS and then placed in 1 ml of chilled mincing solution (HBSS, Ca^{++}, Mg^{++} free, 20 mM Na_2EDTA, 10% DMSO, pH 7.5). After 15 min, the supernatant was centrifuged for 10 min at 1000 *g*. Assessment of cell viability in individual cells was not possible in these experimental conditions, because cell membranes were disrupted during the mincing process (Singh et al. *1995*). The occurrence of neuronal death was ruled out by hematoxylin and eosin (H&E) staining and electron microscopic observations (see below).

The pellet obtained was mixed with 75 µl 0.5% low melting-point agarose (prepared in $Ca^{++}Mg^{++}$-free PBS) and layered on conventional slides, pre-dipped in 1% normal melting point agarose (Klaude et al. *1996*). Then, a third layer of 85-µl low melting-point agarose was added. Slides were immersed in ice-cold freshly prepared lysis solution (2.5 M NaCl, 100 mM Na_2EDTA, 10 mM Tris-HCl, 1% Triton X-100 and DMSO 10%, pH 10) to lyse the cells and allow DNA unfolding.

Primary DNA damage

After rinsing in distilled water, slides were placed in a horizontal gel electrophoresis tray and covered with fresh electrophoresis buffer (0.075 M NaOH, 1 mM EDTA, pH>13) for 20 min, to allow DNA unwinding. Electrophoresis was run at 25 V, 300 mA, 20 min at pH>13 to reveal strand breaks and alkaline labile sites (Miyamae et al. *1997*). Slides were then neutralized with 0.4 M Tris for 5 min, immersed in 100% cold methanol for 3 min and air dried. Slides were then stained with ethidium bromide and nuclei were individually observed. For each mouse a total of at least 100 nigral and striatal cells were scored, and the mean was calculated.

Nuclei were observed under a fluorescence microscope (200×), and an image analyzer (Kinetic Imaging Ltd, Komet, version 4) was used to evaluate the percentage of DNA migrated in the tail of the comets. The percentage of tail DNA varies according to the

degree of genetic damage as shown in Fig. 3, where classes ranging from 0.5% up to 99% of migrated DNA are reported.

Oxidative DNA damage

The evaluation of DNA-oxidized bases was carried out by digesting with the lesion-specific repair enzyme endonuclease-III (ENDO-III, kindly provided by Dr. A.R. Collins, Aberdeen, UK), which is able to recognize altered pyrimidines and induce strand breaks in the sugar-phosphate bone at sites of oxidative damage. Enzyme (2 µl) was diluted in 2 ml of buffer solution (0.5 mM Na_2EDTA, 0.1 M KCl, 0.2 mg/ml bovine serum albumin, 40 mM HEPES, pH 8).

Slides undergoing lysis were treated with a total of 50 µl of enzyme solution (or buffer alone, as control), then were incubated at 37°C, for 45 min and electrophorezed.

Morphology

Under i.p. chloral hydrate anesthesia, mice were perfused with 2% paraformaldehyde/0.1% glutaraldehyde in PBS. For light microscopy, 20-microm-thick cryostat sections were processed for cresyl violet, H&E and immunocytochemistry, while, for electron microscopy, after perfusion, brains were maintained in situ overnight at 4°C in the same solution. Striatal samples (0.4 mm^3) were dissected, as a coronal section, from which the surrounding white matter and cortex were removed. The substantia nigra was dissected by micro-punching. Specimens were post-fixed for 2 h, at 4°C in 1% buffered OsO_4, dehydrated in ethanol, and embedded in Epon-Araldite. Sections were then observed under a Jeol JEM 100 SX transmission electron microscope.

Immunocytochemistry

We used rat primary antibodies (Ab I) against DA transporter (DAT), rabbit Ab I against glutamic acid decarboxylase (GAD) 67, rabbit Ab I against vesicular monoamine transporter-2 (VMAT-2), mouse Ab I against serotonin transporter (SERT) obtained from Chemicon International, Temecula, CA, mouse Ab I against tyrosine hydroxylase (TH), rabbit Ab I against glial fibrillary acidic protein (GFAP), rabbit Ab I against ubiquitin, mouse Ab I against HSP-70, obtained from Sigma Chemical Co. (St. Louis, Missouri). For light microscopy, dilutions of Ab I against DAT, TH, GAD 67 and SERT were 1:1000, while Ab I against HSP-70 were diluted 1:500, Ab I against VMAT-2 were diluted 1:300,

and Ab I against ubiquitin 1:100. The secondary biotynilated antibodies (Vector Laboratories, Burlingame, CA) were used at a dilution of 1:200, followed by incubation with Avidin-Biotin Complex kit and diaminobenzydine (Vector). The secondary fluorochrome antibodies (Chemicon) were used at a dilution of 1:400. Sections were observed using a Wetzlar Orthoplan (Leitz) light microscope.

Post-embedding immunoelectron microscopy was carried out on ultrathin sections. All primary antibodies were diluted 1:100 except for HSP-70 (1:50). Then, sections were incubated with gold-conjugated secondary antibodies (Sigma, gold particles: 10–15 nm) diluted 1:50. Alternatively, free-floating sections were processed for pre-embedding immunoelectron microscopy. Ab I were diluted at 1:50 and revealed by diaminobenzidine. All samples were stained with uranyl acetate and lead citrate and examined at transmission electron microscope. For neuronal inclusions, as well as HSP-70 immunogold particles (HSIPs), we carried out a quantitative analysis (see below).

In vitro experiments

Cell cultures and treatments

The rat pheochromocytoma cell line PC12 (American Type Culture Collection) was grown in RPMI 1640 medium supplemented with heat-inactivated 10% horse serum, 5% fetal bovine serum including penicillin (50 IU/ml) and streptomycin (50 mg/ml). Cells were grown in 75-cm^2 flasks and maintained in a humidified atmosphere of 5% CO_2 at 37°C. The medium was changed every 3 days and maintained at the culture conditions described above. Experiments took place during the log-phase of cell growth. At this time point, PC12 cells were seeded in 6-well plates at 5×10^5 cells at a final volume of 1 ml/well and incubated at 37°C in 5% CO_2 for 72 h.

MDMA solutions were prepared by dissolving the powder in saline as a 1-mM stock solution, which was freshly diluted in the culture medium. Pilot experiments, using MDMA concentrations ranging between 1 micro-M and 100 micro-M, were carried out. The dose of MDMA 100 micro-M was selected for the time-course study (4, 12, 24, 72 and 168 h). For electron microscopy, PC12 cells were centrifuged (1000 g × 5 min), fixed (2% paraformaldehyde/0.1% glutaraldehyde in PBS), post-fixed (1% OsO_4 in buffered solution) and routinely processed. For light microscopy, pellets were dissolved in buffer, applied on glass slides by cytospin (12,000 *g* × 10 min), and processed for various stainings.

Western blot

At 24-h and 168-h time points after treatment with MDMA (100 micro-M), PC12 cells were lysed in TEN buffer (50 mM Tris, 2 mM EDTA, 150 mM NaCl, 1% NP-40, pH 7.6, containing 0.1% PMSF and 10 micro-g/ml of protease inhibitors) and centrifuged at 20,600×*g* for 20 min at 4°C. The supernatants were retained and the protein concentration of the supernatant was determined using a protein assay kit (Sigma). Gel electrophoresis was carried out on 10% sodium dodecyl sulfate-polyacrylamide gel from dissolved samples containing 25 micro-g total protein. Following electrophoresis, the proteins were transferred to nitrocellulose membrane (Millipore). The membrane was immersed at 4°C overnight in blocking solution (0.3% not fat dried milk in 20 mM Tris, 137 mM NaCl, pH 7.6 containing 0.05% Tween-20) on an orbital shaker. Subsequently, the membrane was incubated with primary antibody anti-HSP-70 (1:500) for 1 h at room temperature. Blot was probed with horseradish peroxidase-labeled secondary antibody (1:600) and HSP-70 bands were visualized with enhanced chemiluminescence reagents (Amersham Pharmacia Biotech).

Statistical analysis

For biochemical assay, results from control and treated mice were expressed as the mean±SEM of values obtained from groups of 7–10 mice. The effects of MDMA on DA and metabolites were compared using Student''s *t*-test.

For counting inclusions, we measured either cytosolic or nuclear inclusions out of the total number of neurons under observation. A similar sampling was followed to measure HSIPs in the nucleus and cytoplasm. In particular, from each mouse (*n*=7–10) per group, we randomly chose four tissue blocks dissected from substantia nigra or dorso-lateral striatum. From each block, we obtained a number of grids, each one containing several non-serial (for the striatum, size interval =50 microm; for the substantia nigra, size interval = 10 micro-m) slices to count a total of 2000 striatal and 400 nigral cells. In PC12 cell cultures, HSIPs were counted from 100 cells per dish from 10 sister dishes (total number of 1000 cells) administered MDMA or saline.

Data concerning the percentage of whorled inclusions or HSIPs in the cytosol or the nucleus of striatal, nigral and PC12 cells were compared using Student''s *t*-test.

For the comet assay, four parallel tests were performed for each experimental point for a total of at least 100 cells. Data were analyzed using multifactor analysis of variance.

Results

Striatum

Monoamine toxicity

Systemic administration of MDMA to mice (5 mg/kg, ×4, 2 h apart) produced, 7 days later, loss of DA and 5HT terminals in the striatum, as mirrored by the reduction in the striatal levels of DA (Fig. 2A) and its metabolite dihydroxyphenylacetic acid (DOPAC, Fig. 2B) as well as 5HT (Fig. 2C) and its metabolite 5-hydroxyindolaacetic acid (5-HIAA, Fig. 2D). The immunostaining for striatal TH observed in control (Fig. 2E) was markedly reduced following MDMA (Fig. 2F) as measured by semiquantitative densitometric analysis (Fig. 2G). Similarly, following MDMA, we found a decrease of striatal DAT (Fig. 2H, I, in control and MDMA, respectively). The immunostaining for SERT in the striatum of control was also reduced following MDMA, as shown by representative micrographs (Fig. 2J and Fig. 2K, respectively). When SERT immunoreactive structures were counted in 100 slides from striata of MDMA-treated mice, we observed a significant reduction compared with the mean counted in 100 slides from controls (0.068±0.006 SERT immunoreactive stuctures/micro-m^2 compared with 0.132±0.005 SERT immunoreactive stuctures/micro-m^2, respectively). The VMAT-2 immunostaining was also reduced following MDMA, as shown in Fig. 2L, M.

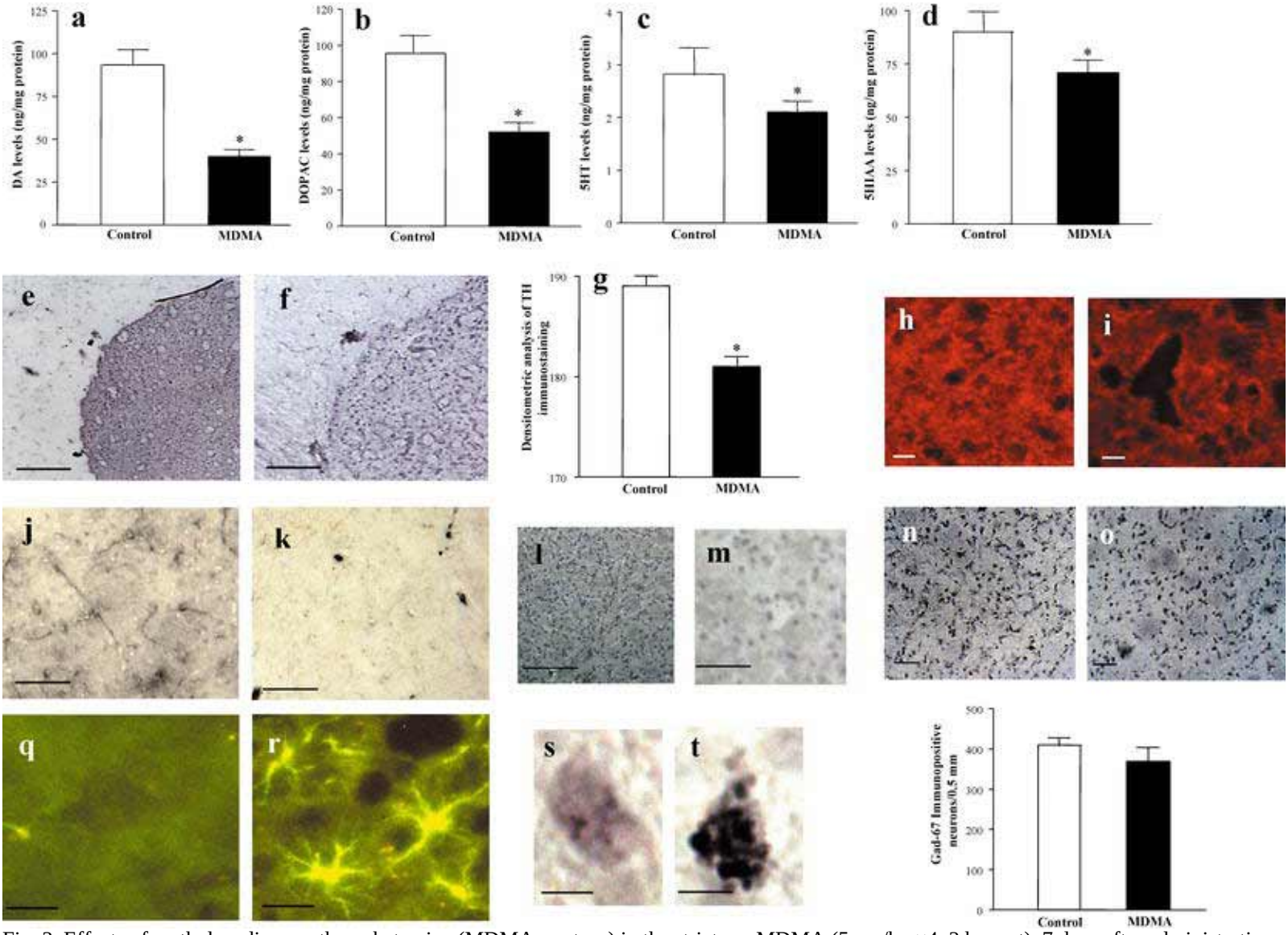

Fig. 2 Effects of methylenedioxymethamphetamine (MDMA; ecstasy) in the striatum. MDMA (5 mg/kg ×4, 2 h apart), 7 days after administration, produces a loss of striatal dopamine (DA) (**a**), dihydroxyphenylacetic acid (DOPAC) (**b**), serotonin (5HT) (**c**) and 5-hydroxyindolaacetic acid (5HIAA) (**d**) levels compared with saline-injected controls. Representative immunohistochemistry of striatal tyrosine hydroxylase (TH) in a control mouse (**e**) is compared with that following MDMA (**f**). Semiquantitative densitometry for TH immunostaining (**g**) confirms that MDMA produces a significant loss of DA terminals. Similarly, representative immunofluorescence indicates that dense fluorescence observed in the striatum of a control mouse (**h**) is markedly reduced following MDMA (**i**). Serotonin transporter (SERT) immunoreactivity from control (**j**) undergoes a reduction following MDMA (**k**). In a similar way, there is a decrease of vesicular monoamine transporter-2 (VMAT-2) immunostaining present in control (**l**) in the striatum of a mouse injected with MDMA (**m**). Representative immunohistochemistry of glutamic acid decarboxylase (GAD) 67 shows no difference between control (**n**) and MDMA (**o**), as confirmed by GAD 67 immunopositive cell count (**p**). However, glial fibrillary acidic protein (GFAP) immunofluorescence is very mild in control (**q**), while following MDMA shows an intense glial immunoreactivity (**r**). MDMA administration produces granular ubiquitin immunostaining within striatal cells (**t**), which does not occur in control (**s**).Values are means±SEM of ten determinations. Semiquantitative densitometry for TH immunostaining was carried out on ten comparable sections from seven mice per group. Cell count of GAD-67 immunostained striatal neurons represents the mean±SEM of five comparable sections from five mice per group. **P*<0.05 (student"s *t*-test) compared with saline. *Scale bars* **e**; **f** = 100 micro-m; **h**; **i** =38 micro-m; **j**; **k** =50 micro-m; **l**; **m**=30 micro-m; **n**; **o** =45 micro-m; **q**; **r** =25 micro-m; **s**; **t** =10 micro-m

Effects on cell bodies

No reduction was found in the number of striatal GABA neurons (Fig. 2N–P) and striatal cell bodies counted following cresyl violet histochemistry (not shown). As commonly observed following damage to striatal nerve endings, striatal astrocytes from MDMA-treated mice possessed higher expression of GFAP along the cell bodies and short branches (Fig. 2Q, R for MDMA and control, respectively). Ubiquitin antibodies revealed the presence of granular immunostaining within the striatal cells of MDMA-treated mice (Fig. 2Q, R, for control and MDMA, respectively), which was further confirmed in nigral cells (see below, and Fig. 3) and analyzed in depth showing ubiquitin-positive intracellular inclusions by electron microscopy (see below, and Fig. 4).

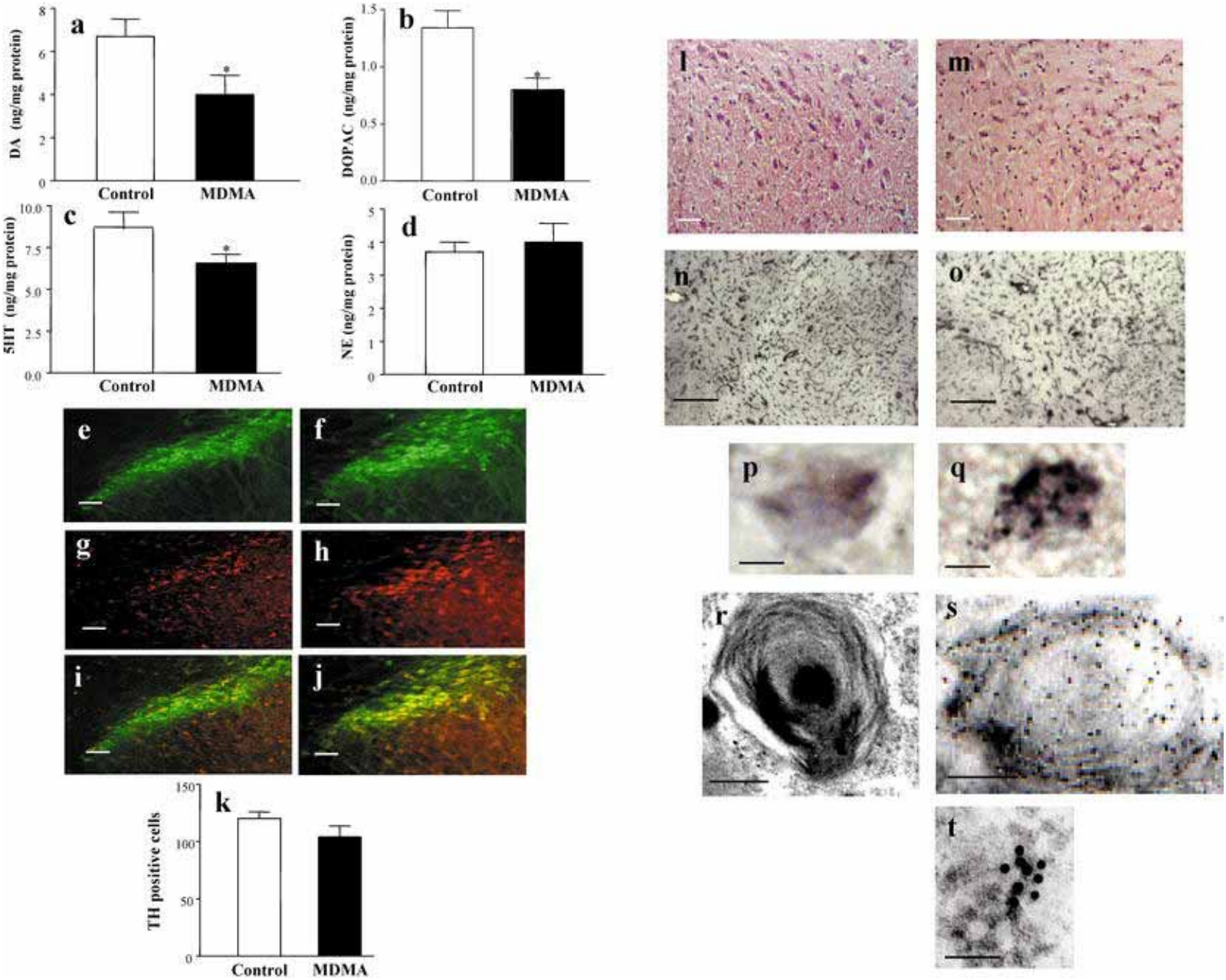

Fig. 3 Effects of methylenedioxymethamphetamine (MDMA; ecstasy) in the substantia nigra. MDMA (5 mg/kg ×4, 2 h apart), 7 days after administration, produces a significant loss of nigral dopamine (DA) (**a**), dihydroxyphenylacetic acid (DOPAC) (**b**) and serotonin (5HT) (**c**), while the levels of norepinephrine (NE) were left intact (**d**). In contrast, no differences were measured in the number of tyrosine hydroxylase (TH) immunopositive nigral cell bodies between control (**e**) and MDMA (**f**), although ubiquitin immunostaining, which is visible in the substantia nigra of control (**g**), increases following MDMA(**h**) showing a co-localization at the level of nigral DA neurons as shown by merging TH and ubiquitin immunostaining in control (**i**) and MDMA (**j**). Nonetheless, cell count of TH immunopositive neurons demonstrate the absence of cell loss (**k**). This is also substantiated by similar number of H&E stained nigral cells as shown in representative micrographs from control (**l**) and MDMA (**m**). No differences in serotonin transporter (SERT) immunostaining between control (**n**) and MDMA (**o**) are detectable at nigral level. When observed at higher magnification, nigral DA neurons already described above (**e**–**j**) show granular ubiquitin immunostaining following MDMA (**q**) but not in controls (**p**). When these neurons from MDMA-treated mice are examined at sub-cellular level, electron microscopy reveals neuronal inclusions shaped as multimembraneous whorls (**r**), in which ubiquitin immunostaining is clustered (**s**). In the cell nucleus of these neurons HSP-70 immunogold particles (HSIPs) cluster close to chromatin (**t**). **P*<0.05 (student"s *t*-test) compared with saline. *Scale bars* **e**–**j** =30 micro-m;**l**; **m** =50 micro-m; **n; o** =25 micro-m; **p**; **q** =15 micro-m; **r** =550 nm; **s** =650 nm; **t** =100 nm

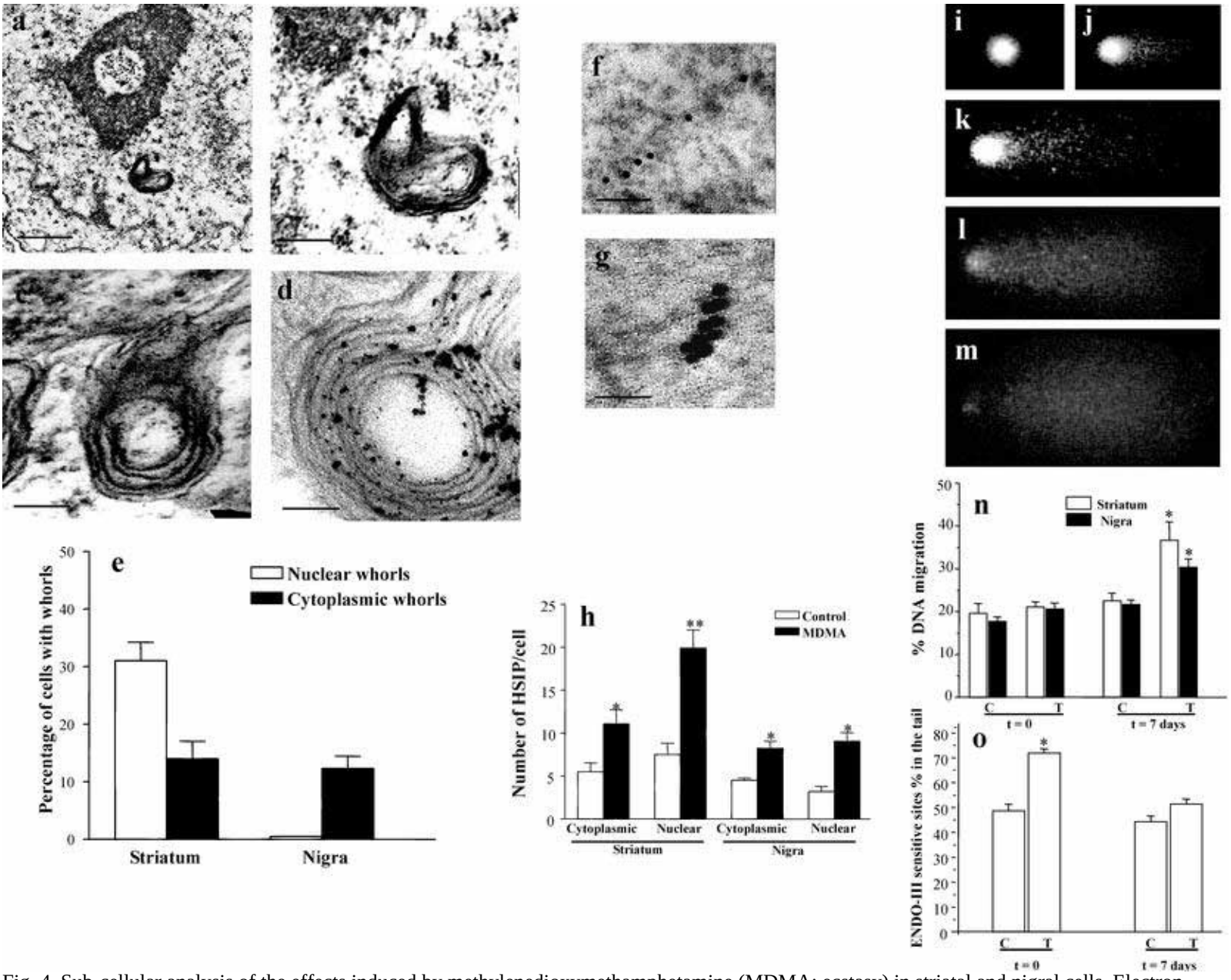

Fig. 4 Sub-cellular analysis of the effects induced by methylenedioxymethamphetamine (MDMA; ecstasy) in striatal and nigral cells. Electron microscopy reveals intraneuronal inclusions consisting of membranous whorls in the nucleoplasm of striatal neurons (**a**, **b** low and high magnification, respectively). In the cytoplasm of striatal neurons, similar inclusions (**c**) are markedly stained for ubiquitin (**d**). Measurement of MDMA-induced whorls within the nucleus of striatal cells and cytoplasm of both striatal and nigral neurons (**e**). Following MDMA administration, within striatal nuclei clusters of HSP 70 immunogold particles (HSIPs) can be observed at different magnification (**f** and **g**). Increase of HSIPs following MDMA occurs both in the nucleus and cytoplasm of striatal and nigral cells (**h**). MDMA administration produces DNA damage both in the striatum and nigra (**i–o**). The DNA damage is shown by representative electrophoresis migration of ethidium bromide-stained nuclei of striatal cells (**i**: 0.5%, **j**: 10%,**k**: 45%, **l**: 93%, **m**: 99%; % = percentage of DNA migrated in the tail). Measurements of DNA migration, demonstrate that at the end of MDMA binging (6 h after the first administration) no differences between treated and control samples are observed in the striatum and substantia nigra concerning primary DNA damage. However, the primary damage is significant at 7 days after treatment (**n**). In contrast, immediately after MDMA binging, a significant oxidation to DNA bases (ENDO-III sensitive sites) is present, while this is no longer detectable at 7 days after treatment (**o**). **P*<0.05 compared with control. ***P*<0.001 compared with control. *Scale bars* **a** =1500 nm; **b**= 500 nm; **c**; **d** =800 nm; **f** =200 nm; **g** =50 nm

Substantia nigra

MDMA administration decreased significantly nigral levels of DA (Fig. 3A) and its metabolite DOPAC (Fig. 3B); a slight reduction was measured for the monoamine 5HT (Fig. 3C), while the levels of norepinephrine were left intact (Fig. 3D). These biochemical effects were not accompanied by a decrease in the number of DA-containing cell bodies as demonstrated by the picture of TH-immunopositive nigral neurons (Fig. 3E, F), which were also stained for ubiquitin antibodies (Fig. 3G, H). In particular, we found a remarkable co-localization of ubiquitin immunostaining in the substantia nigra at the level of DA neurons as appearing in representative micrographs (Fig. 3I, J), showing merging of TH and ubiquitin immunstaining in the pars compacta in control and following MDMA, respectively. As shown above, no cell loss was counted in DA cell bodies (Fig. 3K). The absence of neurotoxicity (i.e., cell loss) was further confirmed by H&E histochemistry (Fig. 3L, M) while, differing from the striatum, there was no alteration in immunostaining for nigral SERT (Fig. 3N, O). Therefore, despite significant damage to striatal DA axon terminals, we could not detect any cell loss following MDMA when we examined TH-immunopositive DA cell bodies in the substantia nigra pars compacta. However, as shown above, these neurons were highly ubiquitinated and they possessed dense clusters of ubiquitin immunostaining at higher magnification (Figs. 3P, Q, for control and MDMA, respectively). At electron microscopy, in these nigral neurons from MDMA-treated mice, we observed neuronal inclusions shaped as multimembraneous whorls (Fig. 3R) in which cytoplasmic ubiquitin immunostaining was clustered (Fig. 3S), while the nucleus of these neurons possessed clusters of HSP-70 surrounding chromatin filaments (Fig. 3T).

Fine alterations in striatal and nigral cells

Neuronal inclusions

As previously shown, MDMA administration produces neuronal inclusions shaped as

multilamellar bodies. Inclusions were found in neurons from the pars compacta of the substantia nigra, where they were exclusively localized in the cytoplasm (Fig. 3L, M). In contrast, these structures were present both in the nucleus (Fig. 4A, B) and cytosol (Fig. 4C) of striatal neurons, where similarly to nigral inclusions they possessed rich ubiquitin immunostaining (Fig. 4D). Occurrence of these whorls was comparable in the cytoplasm of striatal and nigral cells (14.13±3% and 12.3±2.1%, respectively), while they involved exclusively the nucleus of striatal neurons (31.02±3.2%) and were never found in the nucleus of nigral cells (Fig. 4E).

Nuclear and cytoplasmic whorls occurring in neurons of the striatum and substantia nigra possessed a comparable size, with a diameter ranging from 0.1 micro-m to 2.4 micro-m.

HSP-70 immunogold particles

Following MDMA administration, both striatal and nigral neurons expressed higher amount of HSP-70. In particular, this oxidative stress-related protein increased also in striatal neurons (Fig. 4F,G as already observed in nigral neurons, Fig. 3T), where we found clusters of HSIPs very close to chromatin filaments. This increase in HSIPs was particularly evident in the nucleus of striatal neurons, although it was present also in nigral cells and involved the cytoplasm (Fig. 4H).

DNA damage

MDMA-induced ubiquitin-positive neuronal inclusions and occurrence of nuclear clusters of HSP-70 was accompanied by a significant increase of primary DNA fragmentation, since we found a comparable damage to DNA in the substantia nigra and striatum (measured as DNA migration under electrophoresis, Fig. 4I–M). This DNA damage, neuronal inclusions and HSIP clusters were documented at 7 days following MDMA administration.

However, when mice were sacrificed at the end of the binging of MDMA (6 h after the first administration), no differences between treated and control samples were observed in the striatum and substantia nigra concerning primary DNA damage (Fig. 4N). In contrast, at this time interval, MDMA produced a significant oxidation to DNA bases measured by migration in the comet tail of ENDO-III sensitive DNA sites (Fig. 4O). Opposite to the effects on primary DNA fragmentation, oxidized DNA bases were no longer detectable at 7 days after treatment (Fig. 4O).

Effects on PC12 cells

In an attempt to reproduce intracellular inclusions in a simple and homogeneous cellular model, we used undifferentiated PC12 cells, which derive from the neural crest and contain catecholamines. PC12 cells exposed to MDMA (100 micro-M) developed granular immunostaining for HSP-70 and ubiquitin compared with controls (Fig. 5A, B and Fig. 5C, D, respectively). When immunoblotting HSP-70, we found that MDMA administration increased the expression of the protein (Fig. 5E), while no increase was observed for ubiquitin (data not shown). Immunoelectron microscopy confirmed occurrence of both nuclear (Fig. 5F) and cytoplasmic (Fig. 5G) clusters of HSIPs in MDMA treated cells. The increase in the number of HSIPs measured by electron microscopy (Fig. 5H) was more pronounced in the nucleus.

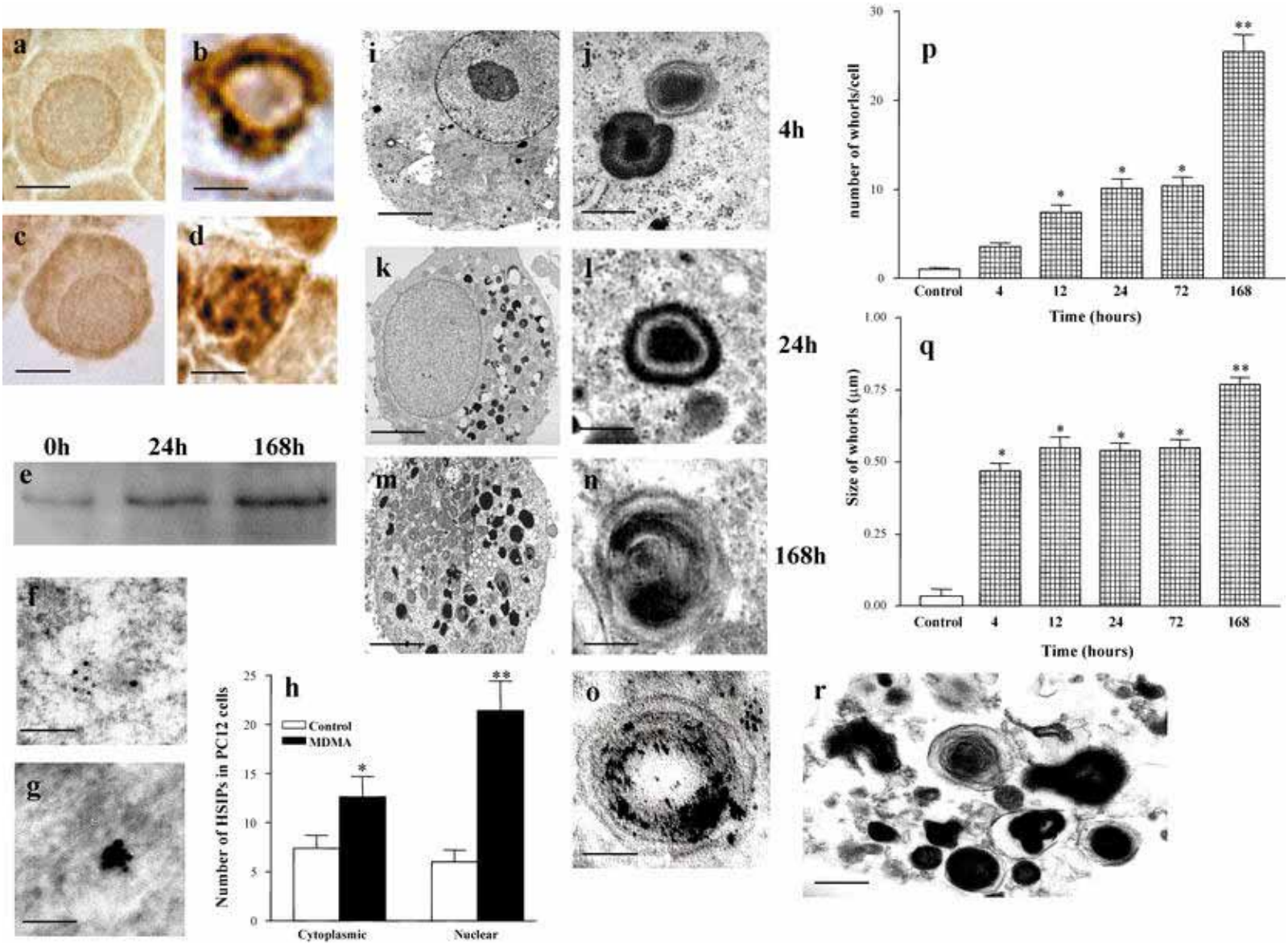

Fig. 5 Fine alterations produced by methylenedioxymethamphetamine (MDMA; ecstasy) in PC12 cell cultures. Control PC12 cell shows a pale and homogeneous ubiquitin immunostaining (**a**) compared with sister cultures exposed to MDMA (100 micro-M) (**b**). Pale HSP-70 immunostaining from a control cell (**c**) versus granular immunopositivity detected in MDMA-treated cell (**d**), in which an increase in the HSP-70 is visible at immunoblotting (**e**). At electron microscopy, HSP-70 immunogold particles (HSIPs) are visible as clusters occurring both in the nucleus (**f**) and cytoplasm (**g**) of MDMA-treated cells. The significant increase of HSIPs we found following MDMA compared with control cultures was more pronounced in the nucleus (**h**). In MDMA-treated PC12 cells there are intracellular inclusions **i**–**n**), which are comparable to those described in the substantia nigra (Fig. 2) and striatum (Fig. 3). The effects of MDMA on PC12 cells are time-dependent (**i**–**n**), with a progressive increase in the concentration of inclusions per cell. As observed in vivo, these inclusions are densely immunostained for ubiquitin (**o**). The time-dependent maturation of inclusions reached a maximum of inclusions per cell at 7 days following MDMA (**p**), when the inclusions became significantly larger (**q**). The presence of analogous inclusions is visible also in the context of disrupting cell membranes (**r**). **P*<0.05 compared with control. ***P*<0.001 compared with control. *Scale bars* **a**–**d** = 4 micro-m; **f**; **g** =200 nm; **i**; **k**; **m** =1500 nm; **j**; **l** =600 nm; **n**; **o** =300 nm; **r** =400 nm

Analytical observation of MDMA-treated PC12 cells revealed intracellular inclusions analogous to those described in the substantia nigra (Fig. 3) and striatum (Fig. 4). The effects of MDMA on PC12 cells was time dependent, with the entire cell population developing the inclusions after 24 h of exposure to 100 micro-M MDMA (not shown). Further, when we examined the cell population at different time intervals following MDMA exposure, we found a progressive increase in the concentration of inclusions per cell (Fig. 5I–N). As observed in vivo, these inclusions occurring in vitro were densely stained for ubiquitin (Fig. 5O). We observed that the concentration reached a maximum of 25.47±1.93 inclusions per cell at 7 days following MDMA (Fig. 5P). Apart from the increased density, these intracellular inclusions augmented progressively their size up to 1 week after MDMA exposure (Fig. 5Q), when we could observe extracellular inclusion bodies surrounded irregularly by cell vestigia (Fig. 5R).

Discussion

The present paper reports effects produced by authentic MDMA as revealed by gas chromatography and analyzed by comparing mass spectra (Fig. 1). We found that MDMA (5 mg/kg ×4, 2 h apart) produces nuclear alterations consisting in DNA oxidation and DNA single-strand breaks accompanied by increased clustering of HSP-70 in the nucleus close to chromatin filaments. We further demonstrate in the cytoplasm and nucleus occurrence of ubiquitin-positive inclusion bodies. Altogether, these findings suggest that MDMA-induced oxidation involves neuronal cell bodies and extends to the nucleus of neurons. These findings were obtained both in substantia nigra and striatum in vivo, and were reproducible in vitro in PC12 cells.

In addition, we observed a loss of striatal DA levels, TH, DAT and VMAT-2 immunostaining accompanied by slight decrease of 5HT levels and SERT immunostaining occurring with increased GFAP immunofluorescence, while no decrease was measured in the number of cell bodies in the substantia nigra. These latter data suggest a clear neurotoxic effect for striatal DA nerve ending concomitant with loss of 5HT makers. Effects of MDMA have been constantly revisited: early evidence indicating selective neurotoxicity for central 5HT neurons (Schmidt *1987*; Finnegan et al. *1988*; Ricaurte et al. *1988*; O"Hearn et al. *1988*) has been extended by recent findings showing that MDMA

neurotoxicity occurs beyond 5HT terminals. For instance, studies carried out in mice (Logan et al. *1988*; Cadet et al. *1995*; O"Shea et al. *2000*; Colado et al. *2001*; Fornai et al. *2001*) demonstrated occurrence of severe DA toxicity following MDMA. In particular, as outlined by Colado et al. (*2001*), when considering mice, DA neurotoxicity is a constant feature of MDMA intoxication. However, 5HT neurotoxicity which is prevalent in rats, in mice has been reported not to occur (Colado et al. *2001*) or is concomitant (Itzhak et al. *2003*) or even if present is less pronounced than DA neurotoxicity (present findings) and other reports (Battaglia et al. *1988*; Fornai et al. *2001*). It is likely that strain differences might play a role in the occurrence of 5HT toxicity in mice as demonstrated by Zheng and Laverty (*1993*) who found that MDMA, besides constant DA loss, produces either no 5HT toxicity or significant 5HT loss, depending on the mouse strain. Apart from slight differences between these studies, there is convergence that, in mice, MDMA behaves as a DA neurotoxin which does not occur in rats.

The present study demonstrates that besides an effect on axon terminals, MDMA administration produces sub-cellular alterations in the neuronal cell bodies. These alterations consist of ubiquitin-positive neuronal inclusions both in substantia nigra and striatum. Striatal inclusions extend to the nucleus of the cell, where we could measure clusters of HSP-70 surrounding chromatin filaments; this was associated with DNA oxidation (measured immediately after the end of MDMA administration) and single strand breaks (detected at 7 days after treatment).

When observed at light microscopy, the number of nigral cells stained for TH, and striatal GABA neurons was not modified by MDMA administration. However, ubiquitin immunostaining revealed the presence of neuronal inclusions, which, when analyzed at transmission electron microscopy, appeared as ubiquitin-positive cytoplasmic (substantia nigra and striatum) and nuclear (striatum) whorls of concentric membranes. These findings demonstrate that MDMA-induced alterations extend beyond a neurotoxicity for axon terminals and involves sub-cellular changes at the level of DA and GABA cell bodies, which undergo sub-cellular alterations reminiscent of neurodegenerative disorders. In order to further characterize MDMA-induced inclusions, we administered MDMA (100 micro-M) to PC12 cell cultures for different time intervals. Occurrence of intracellular aggregates was detected at light microscopy after treating PC12 cells with MDMA for various time intervals. In PC12 cells, we could find ubiquitin-immunopositive inclusions that, when observed at transmission electron microscopy, were similar to those described in vivo, as they appeared as whorls of concentric membranes. Using cell cultures, we followed the dynamic of inclusion formation, which became more abundant and larger by increasing the time of MDMA exposure. In a few cases we were able to detect intact inclusions within cell vestigia surrounded by disrupting cell membranes.

At sub-cellular level, in vivo and in vitro, MDMA-induced nuclear alterations consisted also of clusters of HSIPs which were particularly abundant around chromatin filaments. Again, when using single-cell gel electrophoresis (comet assay), we found striatal and nigral cells undergoing single-strand breaks at 7 days after MDMA administration. Conversely, when we analyzed occurrence of DNA base oxidation, this was significantly increased soon after MDMA injection and no-longer detectable at 7 days. The oxidative alteration of DNA bases gave rise to alkali labile sites and abasic sites, which are known to be transformed in strand breaks during repair processes (Collins et al. *1995*). This mechanism might account for the different timing at which oxidized bases and DNA integrity loss occur.

It is widely known that MDMA administration increases oxidative stress and decreases efficiency of antioxidant systems (Gibb et al. *1990*; Jayanthi et al. *1999*; Green et al. *2003*). DNA base oxidation we observed here might reflect an extension, to the nuclear compartment, of oxidative processes triggered by MDMA. Similarly, this might be the trigger for DNA single-strand breaks detected at 7 days after treatment. Occurrence of ubiquitin-positive nuclear inclusions, associated with clusters of HSIPs close to chromatin filaments and DNA single-strand breaks, altogether clearly demonstrate that MDMA toxicity extends to the nuclear compartment. In fact, HSP-70 is known to play a seminal role in protecting and repairing chromatin filaments (Abe et al. *1995*; States et al. *1996*; Sherman and Goldberg *2001*), which we demonstrated to be damaged by MDMA administration. Besides DNA repair, HSP-70 is important in re-folding and/or degrading misfolded nuclear proteins via the ubiquitin-proteasome system (Sherman and Goldberg *1996*), which is located also in the nucleus (Hershko and Ciechanover *1998*). In keeping with this, the nuclear inclusions we found following MDMA administration were ubiquitin immunopositive, thus suggesting a link between the ubiquitin-proteasome system and early neuronal inclusions, which deserves further investigations. In the cytoplasm of striatal and foremost nigral neurons, degradation of misfolded proteins might occur following a similar pathway and/or involving the autophagic system, as indicated by Larsen et al. (*2002*) for methamphetamine toxicity. Interestingly, these inclusions observed in vivo following MDMA share a similar structure and immunoreactivity with those we recently described in the nigrostriatal system following proteasome inhibitors (Fornai et al. *2003*), thus suggesting a role of an altered ubiquitin proteasome system in the neurological effects induced by MDMA.

The present findings demonstrate that MDMA administration produces in vivo neuronal inclusions and genetic damage both in DA and non-DA (striatal) neurons, raising concerns about the occurrence of a clastogenic effect in chronic MDMA abusers.

References

Abe T, Konishi T, Hirano T, Kasai H, Shimizu K, Kashimura M, Higashi K (1995) Possible correlation between DNA damage induced by hydrogen peroxide and translocation of heat shock 70 protein into the nucleus. Biochem Biophys Res Commun 206:548–555

Battaglia G, Yeh SY, De Souza EB (1988) MDMA-induced neurotoxicity: parameters of degeneration and recovery of brain serotonin neurons. Pharmacol Biochem Behav 29:269–274

Cadet JL, Ladenheim B, Hirata H, Rothman RB, Ali S, Carlson E, Epstein C, Moran TH (1995) Superoxide radicals mediate the biochemical effects of methylenedioxymethamphetamine (MDMA): evidence from using CuZn-superoxide dismutase transgenic mice. Synapse 21:169–176

Colado MI, Camarero J, Mechan AO, Sanchez V, Esteban B, Elliott JM, Green AR (2001) A study of the mechanisms involved in the neurotoxic effects of 3,4 methylenedioxymethamphetamine (MDMA, ecstasy) on dopamine neurones in mouse brain. Br J Pharmacol 134:1711–1723

Collins AR, Ma AG, Duthie SJ (1995) The kinetics of repair of oxidative DNA damage (strand breaks and oxidised pyrimidines) in human cells. Mutat Res 336:69–77

Finnegan KT, Ricaurte GA, Ritchie LD, Irwin I, Peroutka SJ, Langston JW (1988) Orally administered MDMA causes a long-term depletion of serotonin in rat brain. Brain Res 447:141–144

Fornai F, Chen K, Giorgi FS, Gesi M, Alessandrì MG, Shih JC (1999) Striatal dopamine metabolism in monoamine oxidase B-deficient mice: a brain dialysis study. J Neurochem 73:2434–2440

Fornai F, Giorgi FS, Gesi M, Chen K, Alessandrì MG, Shih JC (2001) Biochemical effects of monoamine neurotoxins DSP-4 and MDMA in specific brain regions of MAO-B-deficient mice. Synapse 39:213–221

Fornai F, Lenzi P, Gesi M, Ferrucci M, Lazzeri G, Busceti CL, Ruffoli R, Soldani P, Ruggieri S, Alessandrì MG, Paparelli A (2003) Fine structure and biochemical mechanisms underlying nigrostriatal inclusions and cell death following proteasome inhibitors. J Neurosci 23:8955–8966

Gibb JW, Johnson M, Hanson GR (1990) Neurochemical basis of toxicity. Neurotoxicology 11:317–321

Green AR, Mechan AO, Elliot JM, O"Shea E, Colado MI (2003) The pharmacology and clinical pharmacology of 3,4-methylenedioxymethamphetamine (MDMA, "ecstasy"). Pharmacol Rev 55:463–508

Gudelsky GA, Yamamoto BK (2003) Neuropharmacology and neurotoxicity of 3,4-methylenedioxymethamphetamine. Methods Mol Med 79:55–73

Hershko A, Ciechanover A (1998) The ubiquitin system. Annu Rev Biochem 67:425–479

Itzhak Y, Ali SF, Achat CN, Anderson KL (2003) Relevance of MDMA ("ecstasy")-induced neurotoxicity to long-lasting psychomotor stimulation in mice. Psychopharmacology 166:241–248

Jayanthi S, Ladenheim B, Andrews AM, Cadet JL (1999) Overexpression of human copper/zinc superoxide dismutase in transgenic mice attenuates oxidative stress caused by methylenedioxymethamphetamine (ecstasy). Neuroscience 91:1379–1387

Klaude M, Eriksson S, Nygren J, Ahnstrom G (1996) The comet assay: mechanisms and technical considerations. Mutat Res 363:89–96

Larsen KE, Fon EA, Hastings TG, Edwards RH, Sulzer D (2002) Methamphetamine-induced degeneration of dopaminergic neurons involves autophagy and upregulation of dopamine synthesis. J Neurosci 22:8951–8960

Logan BJ, Laverty R, Sanderson WD, Yee YB (1988) Differences between rats and mice in MDMA (methylenedioxymethamphetamine) neurotoxicity. Eur J Pharmacol 152:227–234

Lyles J, Cadet JL (2003) Methylenedioxymethamphetamine (MDMA, ecstasy) neurotoxicity: cellular and molecular mechanisms. Brain Res Rev 42:155–168

Miyamae Y, Iwasaki K, Kinae N, Tsuda S, Murakami M, Tanaka M, Sasaki YF (1997) Detection of DNA lesions induced by chemical mutagens by the single-cell gel electrophoresis (Comet) assay. 2. Relationship between DNA migration and alkaline conditions. Mutat Res 393:107–113

O"Hearn E, Battaglia G, De Souza EB, Kuhar MJ, Molliver ME (1988) Methylenedioxyamphetamine (MDA) and methylenedioxymethamphetamine (MDMA) cause selective ablation of serotonergic axon terminals in forebrain: immunocytochemical evidence for neurotoxicity. J Neurosci 8:2788–2803

O"Shea E, Esteban B, Camarero J, Green AR, Colado MI (2000) Effect of GBR 12909 and fluoxetine on the acute and long-term changes induced by MDMA ("ecstasy") on the 5HT and dopamine concentrations in mouse brain. Neuropharmacology 40:65–74

Parrott AC, Milani RM, Parmar R, Turner JD (2001) Recreational ecstasy/MDMA and other drug users from U.K. and Italy: psychiatric symptoms and psychobiological problems. Psychopharmacology 159:77–82

Pope HG Jr, Ionescu-Pioggia M, Pope KW (2001) Drug use and life style among college undergraduates: a 30-year longitudinal study. Am J Psychiatry 158:1519–1521

Ricaurte GA, DeLanney LE, Iewin I, Langston JW (1988) Toxic effects of MDMA on central serotonergic neurons in the primate: importance of route and frequency of drug administration. Brain Res 446:165–168

Schmidt CJ (1987) Neurotoxicity of the psychedelic amphetamine, methylenedioxymethamphetamine. J Pharmacol Exp Ther 240:1–7

Sherman MY, Goldberg AL (1996) Involvement of molecular chaperones in intracellular protein breakdown. In: Feige U, Morimoto RI, Yahara I, Polla BS (eds) Stress-inducible cellular response. Birkhauser Verlag, Basel, pp 57–78

Sherman MY, Goldberg AL (2001) Cellular defenses against unfolded proteins: a cell biologist thinks about neurodegenerative diseases. Neuron 29:15–32

Singh NP, McCoy MT, Tice RR, Schneider EL (1988) A simple technique for quantitation of low levels of DNA damage in individual cells. Exp Cell Res 175:184–191

Singh NP, Lai H, Khan A (1995) Ethanol-induced single-strand DNA breaks in rat brain cells. Mutat Res 345:191–196

States BA, Honkaniemi J, Weinstein PR, Sharp FR (1996) DNA fragmentation and HSP70 protein induction in hippocampus and cortex occurs in separate neurons following permanent middle cerebral artery occlusions. J Cereb Blood Flow Metab 16:1165–1175

Strot J, Lee JE, Wechsler H (2002) Increasing MDMA use among college students: results of a national survey. J Adolesc Health 30:64–72

Zheng YW, Laverty R (1993) Neurotoxic effects of MDMA in different strains of mice. Proc Univ Otago Med Sch 71:5–6

Zhou JF, Chen P, Zhou YH, Chen HH (2003) 3,4-Methylenedioxymethamphetamine (MDMA) abuse may cause oxidative stress and potential radical damage. Free Radic Res 37:491–497